

Shake table tests of perimeter-fixed type suspended ceilings

A. Pourali, R.P. Dhakal & G.A. MacRae

Department of Civil and Natural Resources Engineering, University of Canterbury, Christchurch

A.S. Tasligedik

UC Quake Centre, University of Canterbury, Christchurch



2015 NZSEE
Conference

ABSTRACT: This paper reports preparation, execution and preliminary results of a series of shake table tests on perimeter-fixed suspended ceilings, constructed in accordance with the typical New Zealand practice. The tests are conducted in the structures laboratory at University of Canterbury, Civil Engineering Department. The reported ceilings are perimeter-fixed type using the common fix-and-float installation method and are designed for areas of high seismic risk. Through the recorded responses of the ceilings subject to a range of table motions, the relationship between the applied acceleration and the force induced in the ceiling grid members and connections are quantified. The paper reports the effect of the grid members' layout and end-fixing connections on the overall performance of the suspended ceilings. Results of this research will provide basis for the development of simplified design equations to ensure that grid members and connections, whose strengths are known through component tests, do not fail at desired level of floor accelerations.

1 INTRODUCTION

Non-structural elements (NSEs) in building are the components which, despite adding to the design dead loads, do not contribute to the resistance against the design actions (i.e. are not a member of the load path). These elements make up approximately 70% of the total construction cost in commercial buildings (Taghavi 2003) and are often reported as contributing to a significant portion of post-earthquake damage and loss (Dhakal 2010 and 2011).

Suspended ceilings as one of the most common NSEs, are sensitive to acceleration (FEMA 2011). In order to properly evaluate and design these elements, it is therefore necessary to clarify how the imposed ceiling acceleration is transferred among its various components and what proportion of the imposed demand each component carries. Along with the capacity of the ceiling components, the information gathered in this particular work can provide insight into the level of safety of the system under a given demand.

Based on post-earthquakes observations (Dhakal 2010 and 2011), the most common damage types for suspended ceilings are: i) Failure of end rivets in perimeter-fixed ceilings; ii) failure of suspension system at grid intersections; iii) dislodgment and downfall of acoustical tiles due to grid spreading; iv) damage caused by the differential movement of the ceiling relative to vertical structural elements or non-structural elements such as partitions and sprinkler heads and v) failure due to the absence of sufficient bridging and support for other services within or in the vicinity of ceilings, e.g. pipes, ductwork and light fixtures located in ceiling plenum space. In many of the observed cases during recent earthquakes, suspended ceilings suffered significant damage despite the supporting structure sustaining minimal or no damage. This observation indicates an incompatibility between the design and performance requirements for structural and non-structural elements.

Based on these observations, the focus is directed towards the identification of damage states based on accelerations in suspended ceilings. Previous studies (Gilani et al. 2010, Ryu et al. 2012 and Badillo et al. 2007) set criteria describing various damage states and proposed fragility curves for each of these states based on full scale shake table tests.

This paper reports the experimental work conducted on the typical perimeter-fixed suspended ceilings commonly used in New Zealand (Fig.1). These ceilings consist of inverted T-shaped galvanized steel beams that form 1200mm×600mm or 600mm×600mm modules that support ceiling tiles. These T beams are provided in three lengths; Main tees are 3600mm long and cross tees can be 1200mm or 600mm long. The suspension system is hung from the structure above via steel hanger wires or braced to the floor above. On the perimeters the ceiling is either fixed to the structure via rivets and clips or free to slide on wall angles. These ceilings were observed to be prone to damage in recent Christchurch earthquakes and are subject to further study.

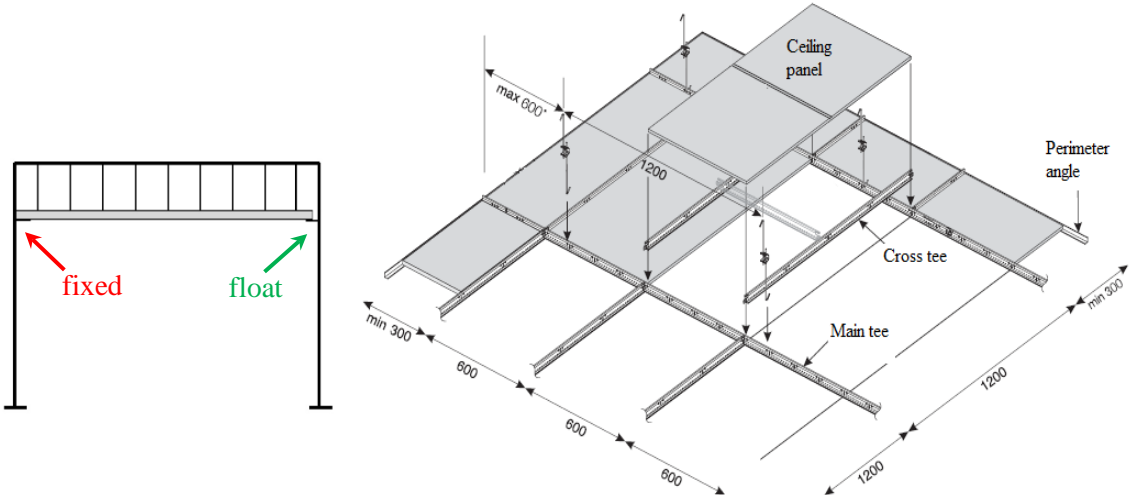


Figure1. Schematic and details of perimeter-fixed ceiling (Armstrong 2013).

The main objectives of the current experiments are:

- Understanding the mechanics of the system including natural properties and demand transfer mechanism among the ceiling components
- Verifying the simple method of estimating connection forces based on peak floor acceleration
- Quantifying the effects of changes applied to the system, such as perimeter fixings

The investigation is based on shake table experiments on full scale suspended ceiling specimens. As shake table functions, sine waves and earthquake ground motions are applied to the specimens. Sinusoidal motions, discussed in this paper, cover various excitation frequencies and amplitudes, which provide a range of results for comparison and overall view. Effects of these parameters are individually investigated and possible interrelationships are identified. For comparison, peak values of acceleration, axial force or displacement in grid members are picked from the time histories, while the infrequent peaks due to the inherent noise caused by the simulation system were ignored.

2 EXPERIMENTS

2.1 Test specimens

Initially, four configurations of ceilings were tested. These specimens are of 2.4m×4.8m size and vary in suspension system layouts (Fig. 2) and end fixing details (Fig. 3) (details provided in Table 1).

Table 1. Details of test specimens

Test Series	Grid loaded	Fixed end	Free end	Tile weight ea. (kg)
Pr-F-A-1	Main tee	3.2mm Rivet	ACM7 clips	2.75
Pr-F-A-2	Main tee	3.2mm Rivet	No clips	2.75
Pr-F-B-1	Cross tee	3.2mm Rivet	ACM7 clips	2.75
Pr-F-B-2	Cross tee	3.2mm Rivet	ACM7 clips	4.63

The first ceiling type referred to as Pr-F-A-1 is shown in Figure 2. In this specimen main tees are in the longitudinal direction and cross tees in transverse direction. ACM7 clips are installed on the free ends of tees allowing tees to slide along their axis (Fig.3). In the second specimen, Pr-F-A-2, the ACM7 clips are removed and grids are free to slide on the seating wall angle. For the third configuration, Pr-F-B-1, a new ceiling was installed in which cross tees were placed in the longitudinal direction and main tees in transverse direction (Fig. 2). The suspension system in this setup was used in the fourth specimen Pr-F-B-2, with heavier tiles replacing the light weight ones. In both specimens Pr-F-B-1 and Pr-F-B-2, ACM7 clips were used on the free ends of grids.

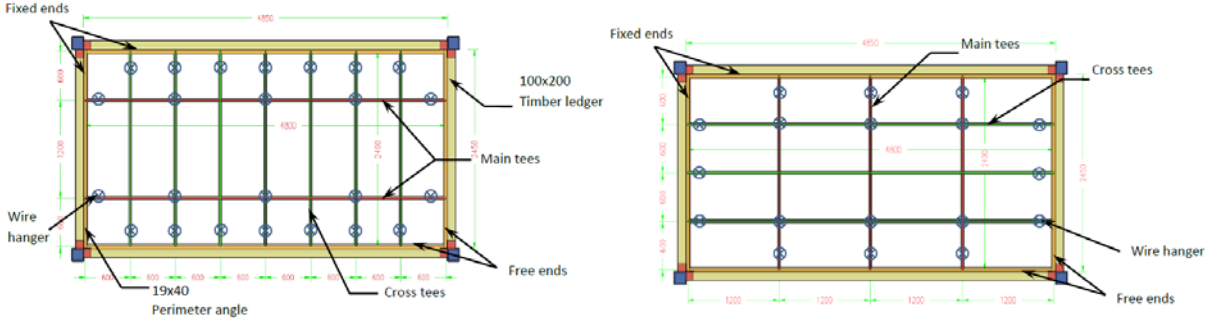


Figure 2. Ceiling specimens Pr-F-A (left) and Pr-F-B (right).



Figure 3. ACM7 clip installed on tee.

2.2 Test setup and instrumentation

The setup was constructed on a 2m by 4m unidirectional earthquake ground motion simulator with an unloaded mass of 5000kg. The shake table has a payload capacity of 20 tonnes and displacement amplitude of 130mm (total stroke of 260mm). The capacity of the servo valves limits the velocity of the table to approximately 242mm/s. This is defined as the saturation velocity of the table, and in all cases, should be avoided (Chase et al. 2005 and Marriott 2009).

The frame erected (Fig.4) is 5.20m long, 2.65m wide and 2.8m high and can accommodate a 2.4m by 4.8m ceiling. The frame is cross-braced in the direction of excitation. Connections at column bases are pinned and rigid fixed end plate connections are used at beam to column joints.



Figure 4. Test frame on shake table.

At ceiling hanging level, 500mm from frame roof, timber beams are fixed to the columns on four sides and 19mm × 40mm wall angles are screwed to the timber beams to provide seating for ceiling tees. Ceiling grids are riveted to these wall angles on two adjacent sides and are free to slide on the two opposite ends.

Suspended ceilings are among the acceleration dependent non-structural elements. As they are located on different elevations inside a building, the imposed demand can significantly vary from the ground acceleration.

For the purpose of this experiment it is most desirable to have an infinitely rigid test frame to simulate the same floor motion at the ceiling level as the one applied to the shake table (ground motion). However, such a frame would be inefficiently heavy and expensive. Therefore, the more reasonable alternative is to use a less rigid frame and consider the ceiling level motion as the input. The frame used in this study is relatively rigid with a horizontal frequency of 12.5Hz. Using a relatively rigid frame ensures that the excitation input to the table is close to what the ceiling is subjected to (i.e. the response excitation of the frame). The relevance of this assumption is later checked through comparison of acceleration output on the shake table, frame and ceiling.

A total of 21 instruments were used for recording the test outputs in the first two series of tests. The number of instruments and their locations were slightly changed in the remaining series as accelerometers with higher capacities were used. A schematic view of the location of these instruments is shown in Figure 3.

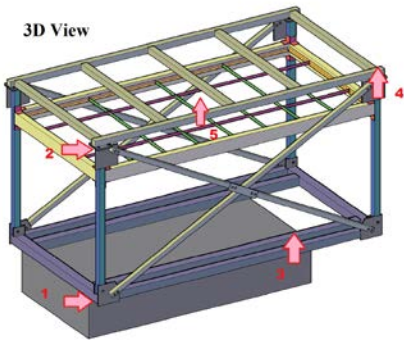
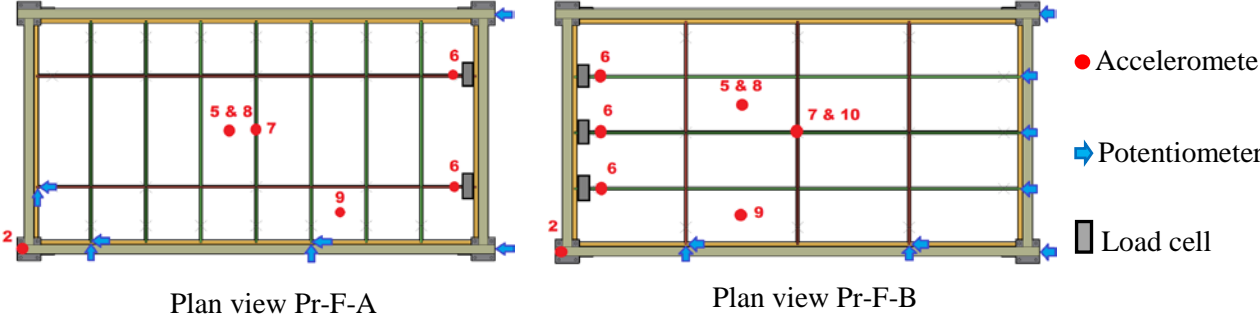


Table 2. List of accelerometers

No.	Location	No.	Location
1	Shake table input (Hrz.)	6	Grid end (Hrz.)
2	Frame top (Hrz.)	7	Central grid (Hrz.)
3	Shake table input (Vrt.)	8	Central tile (Hrz.)
4	Frame top (Vrt.)	9	Perimeter tile (Hrz.)
5	Central tile (Vrt.)	10	Central grid (Vrt.)

Figure 3. Instruments in test series Pr-F-A and Pr-F-B.

2.3 Test input motion

The main objective of these series of tests is to better understand the mechanism in which the suspended ceiling system resists the floor acceleration and how the inertial force is transferred through different components. Therefore, it is more desirable to have a controlled loading regime through which the effect of various parameters of loading can be separately investigated. A series of sinusoidal motions varying in displacement amplitude and frequency were therefore chosen as input motion for these tests. This provides a variety of input PFAs applied on the ceiling. Tables 3 to 5 below show the parameters of motions used for each test series.

Table 3. Details of input motions in test series Pr-F-A-1 and Pr-F-B-1

Frequency of Vibration (Hz)	Displacement Amplitude (mm)	Input acceleration (g)
1	20 & 28	0.08 & 0.11
1.5	20 & 28	0.18 & 0.25
2	12-28 (at 4mm intervals)	0.19 – 0.45
2.5	12-24 (at 4mm intervals)	0.3 – 0.6
3	2-20 (at 2mm intervals)	0.07 – 0.72
3.5	2-16 (at 2mm intervals)	0.1 – 0.8
4	2-12 (at 2mm intervals)	0.13 – 0.77
4.5	2-10 (at 2mm intervals)	0.16 – 0.81
5	2-8 (at 2mm intervals)	0.2 – 0.8

Table 4. Details of input motions in test series Pr-F-B-2

Frequency of Vibration (Hz)	Displacement Amplitude (mm)	Input acceleration (g)
2	12-24 (at 4mm intervals)	0.19 – 0.45
2.5	12-24 (at 4mm intervals)	0.30 – 0.60
3	4-20 (at 2mm intervals)	0.14 – 0.72
3.5	4-16 (at 2mm intervals)	0.20 – 0.79
4	4-10 (at 2mm intervals)	0.26 – 0.64
4.5	2-10 (at 2mm intervals)	0.16 – 0.81
5	3-6 (at 1mm intervals)	0.30 – 0.60

Table 5. Details of input motions in test series Pr-F-A-2

Frequency of Vibration (Hz)	2	3	4
Displacement Amplitude (mm)	12, 16 & 20	2-12 (at 2mm intervals)	4, 6 & 8
Input acceleration (g)	0.19 – 0.32	0.07 – 0.72	0.26 – 0.52

3 RESULTS AND DISCUSSIONS

3.1 Amplification of input motion

Since suspended ceilings are located on different elevations of a building, the value of acceleration applied to them (PFA) is different from the peak acceleration at ground level (PGA). It is also expected that the acceleration applied to the supporting floor is amplified while being transferred to different components of the ceiling. In order to quantify the amount of amplification in the system, comparisons have been made among acceleration outputs at different location of the frame and specimen and presented in Figures 7 to 10.

Figure 7 below shows the amount of amplification in peak horizontal acceleration when transferred from shake table to roof level (Point 2 in Figure 3). The values of amplification are in a reasonably similar range since the two ceilings do not change the properties of supporting frame. Since the frequencies of input motions are far less than the natural frequency of the frame, no significant variation in amplification is observed in different motions. The amplification factors vary from 0.8 to 1.4 and 1.33 in Pr-F-A and Pr-F-B tests respectively.

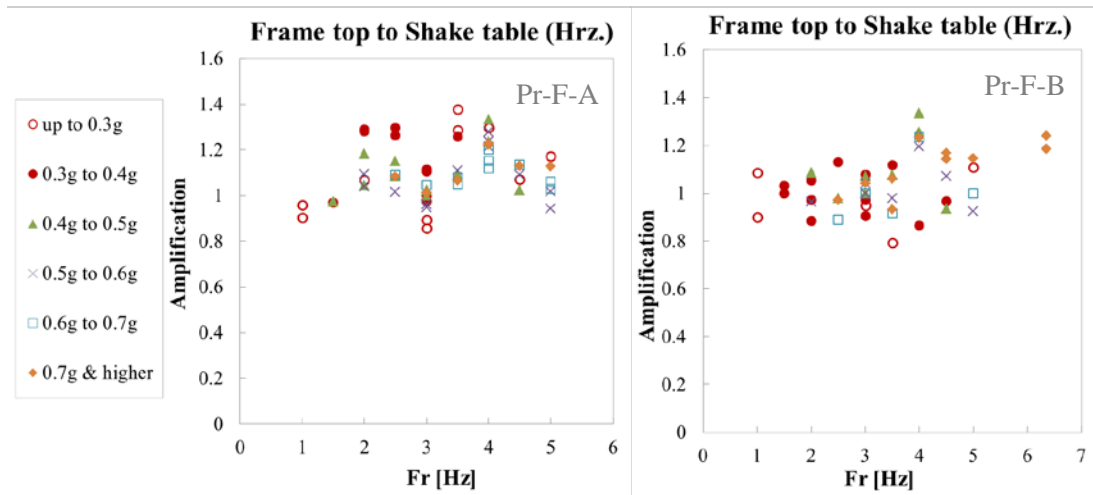


Figure 7. Amplification of input acceleration on frame top.

The acceleration applied at the floor level is transferred to grid members and tiles and is resisted by the end fixing connections. In the next graphs in Figure 8, the values of peak horizontal acceleration recorded on grid members are compared to the peak acceleration at floor level. The values of peak acceleration recorded on grid ends (Point 6 in Figure 3) are 1 to 3.66 times larger than the peak acceleration at the roof level. This amplification varies from 1.25 to 3.8 in central grids (Point 7 in Figure 3).

As it can be observed, higher accelerations generally show a greater level of amplification. However, in case of high frequencies even at a low input level (e.g. around 0.3g), the acceleration induced in grids is much bigger compared to the input and results in a big amplification. The same grid acceleration when induced by a much bigger input excitation (e.g. 0.5g) and lower frequency leads to a smaller amplification factor. Based on these observations, amplification values increase as higher frequencies are applied. These amplifications however show a slight decrease at frequencies higher than 4Hz.

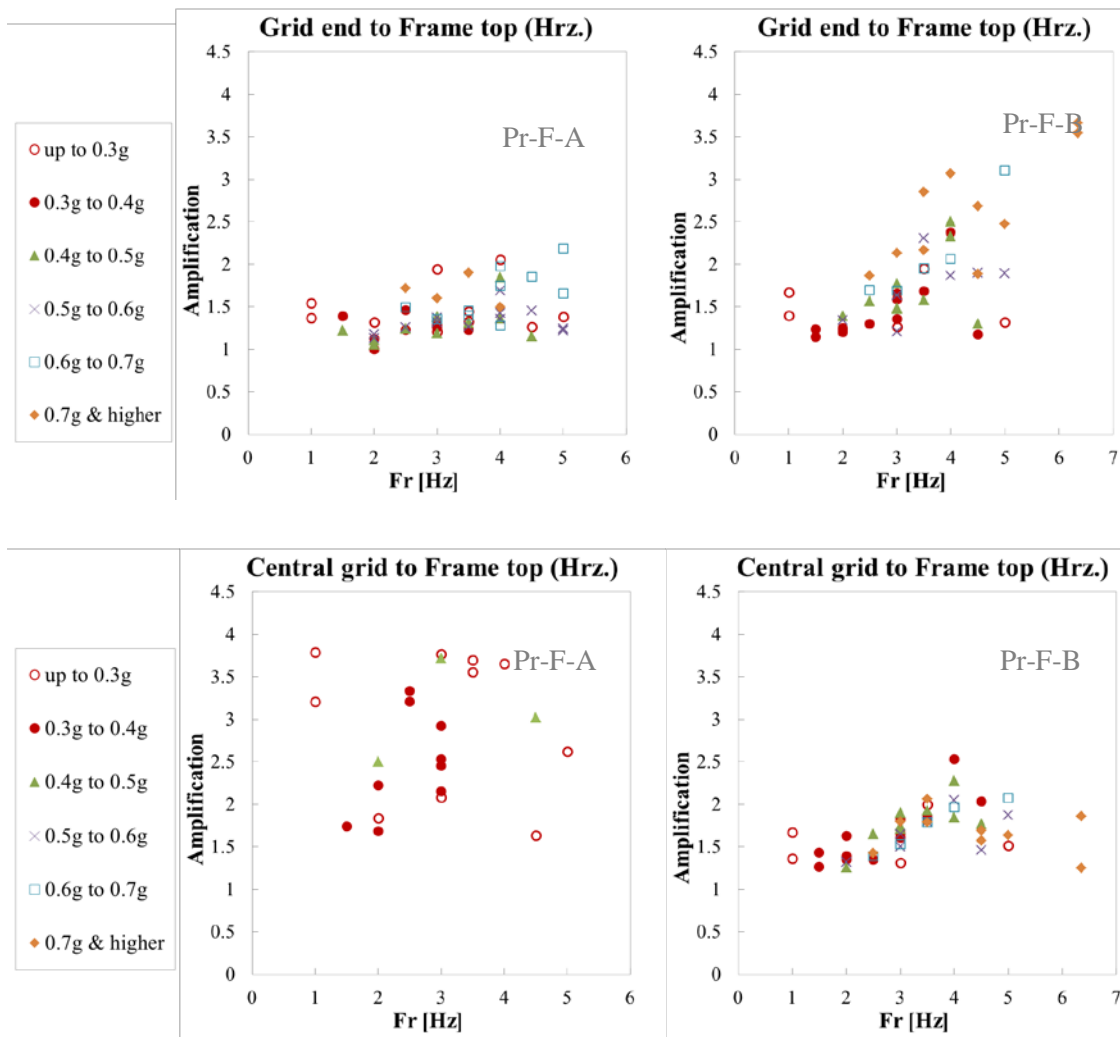


Figure 8. Acceleration amplification factor on grid members

In Pr-F-A tests, the accelerometers recording on grids and tiles reached their capacity and were not recording beyond $\pm 1.5g$. Therefore, a large number of results in these tests were irrelevant and were not included in the graphs. The extent of variation in Pr-F-A is greater compared to Pr-F-B specimen. In Pr-F-B the variation in amplification is 1.25 to 2.53. These differences can be caused by the motions from tiles supported by these grids. The reasons of these discrepancies need to be further investigated in future tests.

Due to the presence of gaps between tiles and the surrounding grids, tiles tend to slide in the modules and in some cases hit the grid members. This excitation is greater in the ceiling centre where large vertical movements were also observed in tiles. As it can be observed in Figure 9, large values of amplification -up to 3.5 times the floor motion- were recorded in central tiles. High amplifications were noticed at frequencies of 3 to 4Hz similar to grid members discussed before.

Regarding the tile size, Pr-F-A ceilings had 600mm \times 600mm tiles on perimeter whereas in Pr-F-B specimens all tiles were 1200mm \times 600mm. Therefore, larger tiles were subject to less movement and showed lower levels of acceleration amplification.

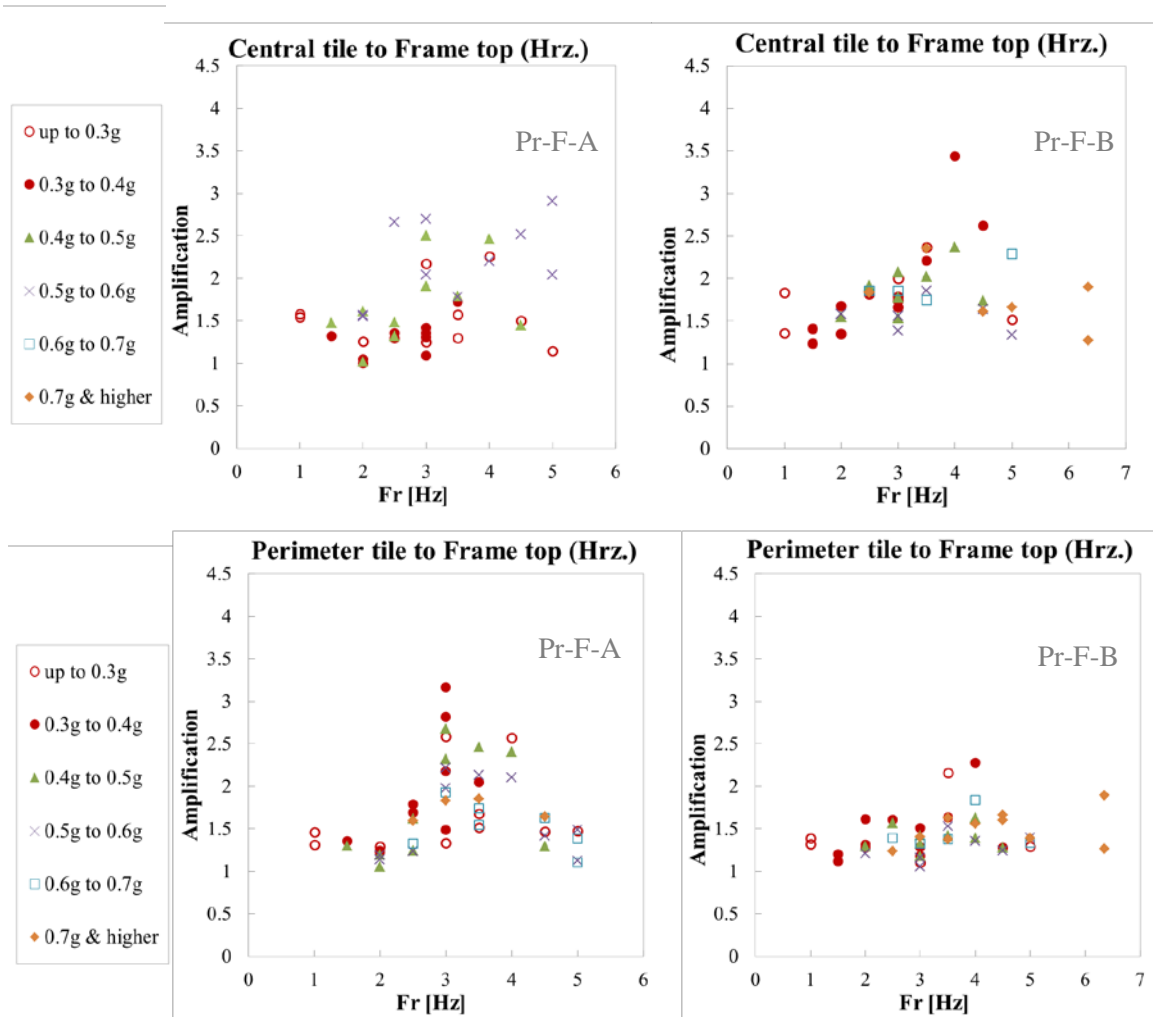


Figure 9. Acceleration amplification factor on tiles.

Based on current codes (NZS 1170.5 2004) the acceleration considered for design of ceilings is amplified using a number of coefficients such as floor height and part spectral shape coefficients. This acceleration applied at the ceiling level can be up to 3.6 times the seismic weight of the part. In case of suspended ceilings which have a natural period of less than 0.75s, the part spectral shape coefficient has a value of 2. This amplification value has been exceeded in graphs provided in Figure 8 which imply that grid members were subject to accelerations up to 3.8 times the peak floor acceleration.

3.2 Force-acceleration relationship

If we assume suspension system to be an elastic grid of beams carrying the seismic force from suspended tiles and supported services, then we can consider the transfer of force through these beams to be linear and cumulative. In other words, this assumption allows us to estimate the inertial force in the end connections as the product of horizontal acceleration and mass associated with the tributary area of the considered beam (Fig. 11). In order to verify this assumption in experiment, load cells and accelerometers were installed at the fixed end of the tees (Fig.10). The axial forces measured by load cells in tees are compared with the product of measured accelerations and mass carried by each beam. These mass values from the associated tributary areas are listed in Table 6 for each test specimen.

Table 6. Mass and tributary area

Test Series	Pr-F-A-1	Pr-F-A-2	Pr-F-B-1	Pr-F-B-2
Area on tee (m ²)	4.8×0.9 = 4.32	4.32	4.8×0.6 = 2.88	2.88
Tile mass (kg/m ²)	3.82	3.82	3.87	6.43
Tributary area mass (kg)	16.5	16.5	11.16	18.52

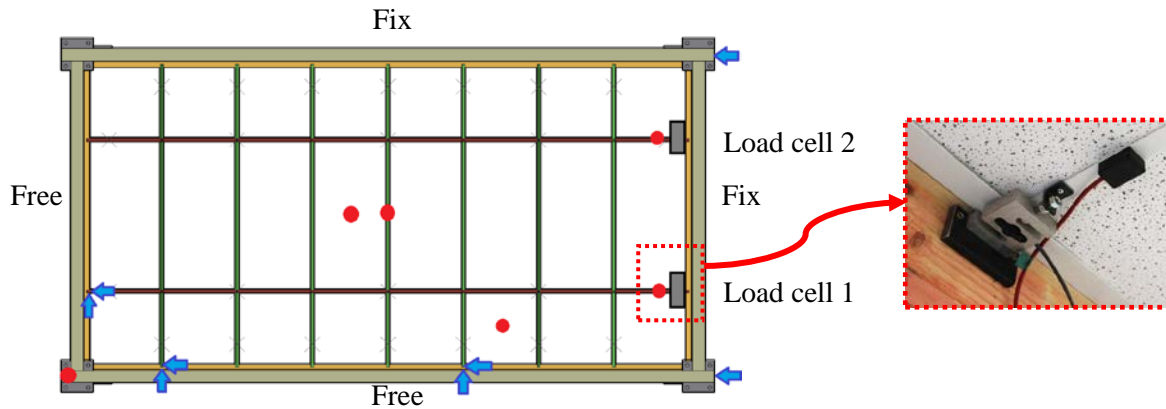


Figure 10 – Layout of instruments and location of load cell on Pr-F-A specimen

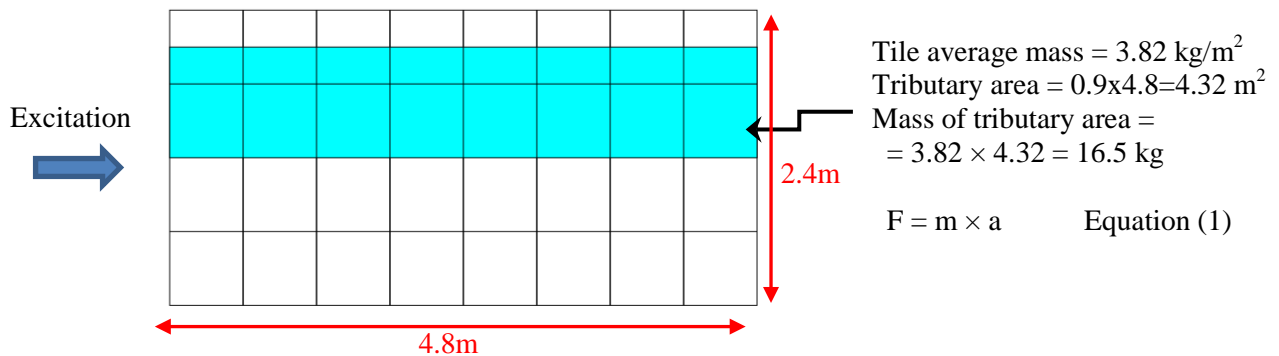


Figure 11. Schematic view of tributary area per main tee.

Figure 12 shows the comparison between the peak force measured by the load cells -solid circles and triangles- and the force calculated as the product of mass and the recorded peak acceleration -hollow circles and triangles. Graphs show positive and negative values of force and acceleration separately. In both graphs, the values of force from load cells are generally lower than what was calculated or expected based on Equation 1. This can be due to the other restraints in the system that affect the load transfer.

In the first order equations shown on the graphs in Figure 12, the slope of each fitted line indicates the mass associated with the grid connected to the load cell. The graphs representing load cell results show a good proximity to the expected values. The highest value of mass i.e. 16.1kg was found on load cell 2 in compression -negative- which is on the fixed-fixed side of the ceiling as shown in Figure 10. This value is the closest to the tributary area mass of 16.5kg in Table 6 -the slope of the hollow figures on graph. The graphs related to the two load cells in tension graphs -positive- follow a more similar trend while load cell 2 still shows bigger values of force and mass. This difference is further discussed in Section 3.3. Since no damage was observed at this stage it can be concluded that the system was still at its elastic stage and the linear assumption is relevant.

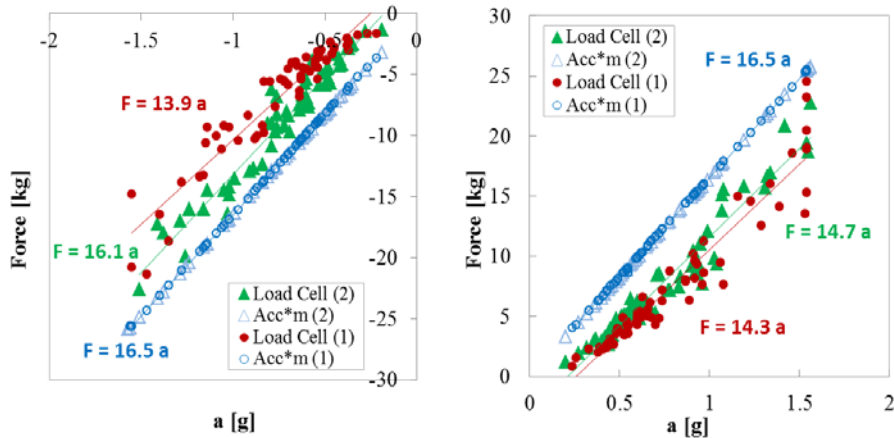


Figure 12. Peak force-acceleration relationship Pr-F-A-1.

Figure 13 is a different way of presenting this data in which values of force measured by load cells are plotted against the values of predicted force based on Equation 1. The first graph is related to series Pr-F-A-1 where ACM7 clips were used on the free ends of grids. This graph shows lower values of force than the second graph where ACM7 clips were removed in series Pr-F-A-2. This comparison shows that applying these end clips increases the rigidity of the end connections on transverse tees, affecting the load transfer in longitudinal tees and leads to the accumulation of a smaller portion of the inertial force in the tee end. Based on the preliminary observations at this stage, these clips resist against rotation and lateral movement of the transverse grids –as they are designed to- reducing the displacement in the longitudinal grid on the free-free side. This comparison is discussed more in Section 3.3.

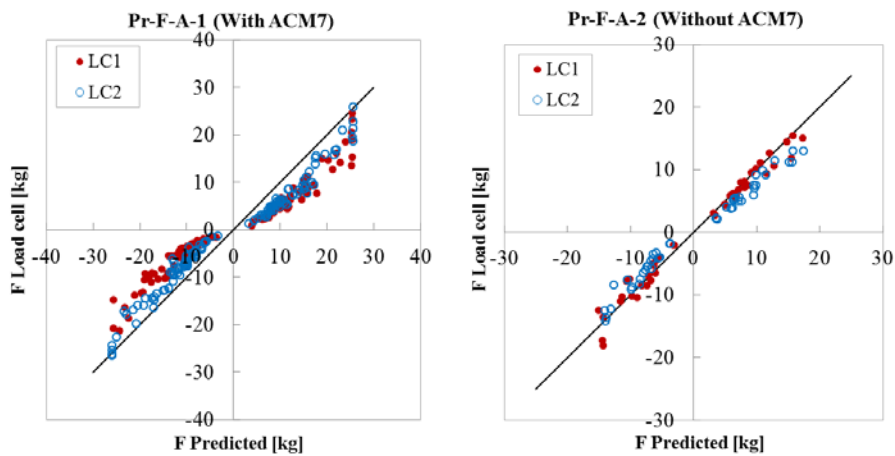


Figure 13. Comparison between recorded and predicted peak force in Pr-F-A ceilings.

3.3 Effect of boundary restraint

Measurement of displacement at the free ends of tees shows that removing ACM7 clips increases the overall motion of the ceiling quite considerably and leads to larger forces in the grid members (Fig. 13).

Figure 14 below compares the displacement of a longitudinal tee for a similar motion when ACM7 clips are installed (a) and removed (b). The grid displacements are plotted along with the frame relative displacement measured at frame top relative to frame floor -in blue- to provide an estimate of the overall effect of clips.

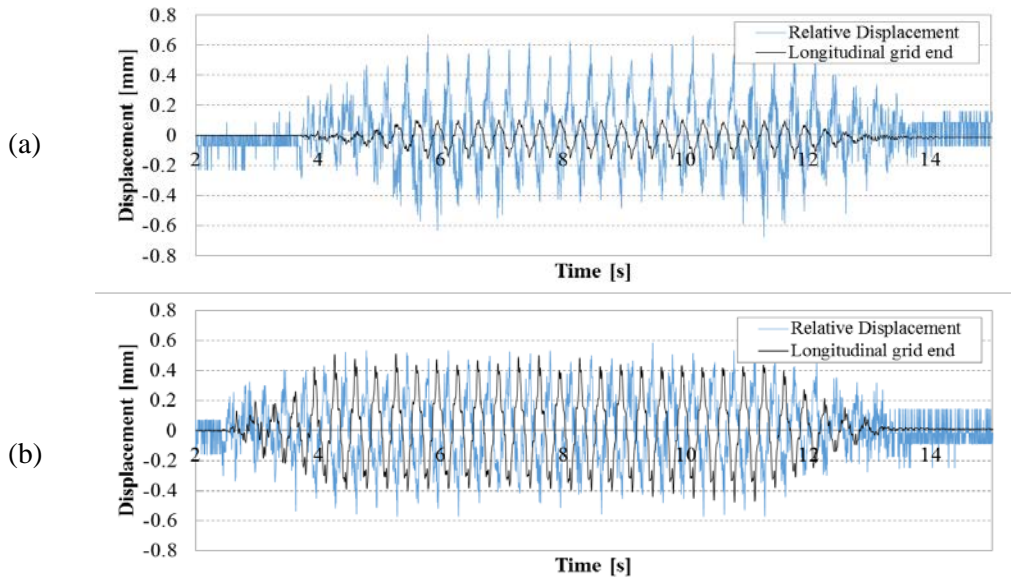


Figure 14. Displacement time histories.

Figure 15 shows an exaggerated schematic view of the assumed rotations and deformations in transverse tees in the two aforementioned specimens. Comparisons between the values of force in two load cells also shows that in Pr-F-A-1 load cell 1 located parallel to the free side (clipped) records smaller values of force than load cell 2 on the riveted side. However in Pr-F-A-2, the values of force recorded by load cell 1 are greater than load cell 2 (Fig. 13). This can be explained by the assumption made about the deformation of transverse tee in two ceilings.

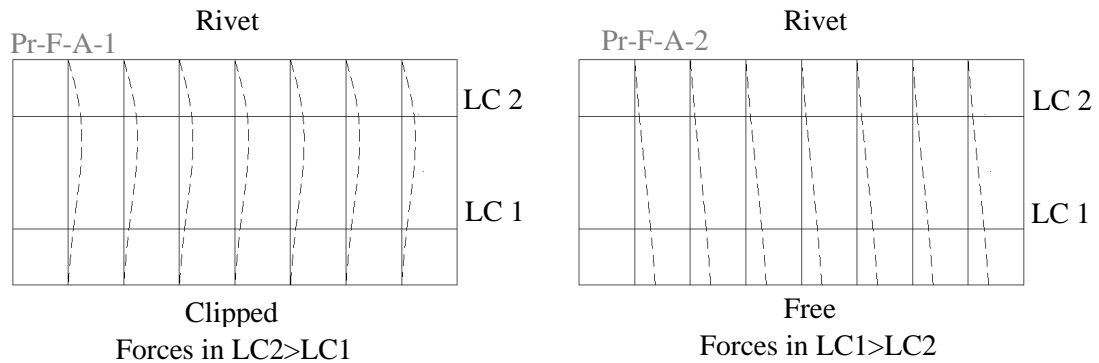


Figure 15. Schematic view of displacement mechanism on grid end with and without clips.

4 CONCLUSIONS

Shake table tests were carried out on two configurations of perimeter-fixed suspended ceilings in University of Canterbury. Specimens varied in grid layout and end fixing type and were subject to sinusoidal motion. Through these experiments, the relevance of the assumption for linear accumulation of inertial forces in grid members in the direction of loading was checked. Based on the preliminary results and observations, the tributary mass concept to relate grid axial forces with ceiling acceleration seems reasonable. However, further investigation is required regarding the effect of system's flexibility and connection types on the effective tributary mass.

The amplification of the input acceleration was also investigated in various components of the system including the test frame, grid members and tiles. These amplification factors vary in different locations of the system but appear to be also dependent on the frequency and amplitude of excitation. The study indicates the significance of the ceiling acceleration estimation in comparison with the code provisions for floor acceleration. Further investigation is required to address the level of amplification applied to

floor acceleration as it is transferred to ceiling grids. It must be noted that these conclusions are based on the preliminary observations of the authors at this stage of the experiment and are therefore subject to change as new experimental work is carried out.

5 ACKNOWLEDGEMENT

This research is supported by The Natural Hazard Platform Research on Non-structural Elements. The authors acknowledge the great contributions of John Maley, UC Structures lab technician, in the constructions of test setup and conduction of shake table tests, and Steve Clements in the installation of suspended ceilings.

6 REFERENCES

- Armstrong. 2013. Armstrong Seismic Design Guide New Zealand Version.
- Badillo-Almaraz, H., Whittaker, A. S., & Reinhorn, A. M. 2007. Seismic Fragility of Suspended Ceiling Systems. *Earthquake Spectra*, 23(1): 21–40. doi:10.1193/1.2357626
- Chase, J.G., Hudson, N.H., Lin, J., Elliot, R. & Sim, A. 2005. Nonlinear shake table identification and control for near-field earthquake testing, *Journal of Earthquake Engineering*, 9(4): 461-482
- Dhakal, R.P. 2010. Damage to non-structural components and contents in 2010 Darfield earthquake, 1–8.
- Dhakal, R.P., MacRae, G.A., & Hogg, K. 2011. Performance of ceilings in the February 2011 Christchurch earthquake, 44(4), 379–389.
- FEMA. 2011. FEMA E74-Reducing the Risks of Nonstructural Earthquake Damage – A Practical Guide.
- Gilani, A. S. J., Reinhorn, A. M., Glasgow, B., Lavan, O., & Miyamoto, H. K. 2010. Earthquake Simulator Testing and Seismic Evaluation of Suspended Ceilings. *Journal of architectural engineering* © ASCE / JUNE 2010, (June), 63–73.
- Marriott, D. 2009. The development of high-performance post-tensioned rocking systems for the seismic design of structures, Thesis.
- Ryu, K. P., Reinhorn, A. M., & Filiatrault, A. 2012. Full Scale Dynamic Testing of Large Area Suspended Ceiling System. In 15 WCEE 2012 (Vol. 1).
- Standards New Zealand, 2004, NZS1170.5:2004 Structural Design Actions Part 5: Earthquake Actions – New Zealand, Wellington, NZ.
- Taghavi, S. & Miranda, E. 2003. Response assessment of nonstructural building elements. PEER-College of Engineering, University of California Berkeley, USA.
- USG. 2012. Generic Seismic Design for USG DONN exposed grid suspended ceilings.